

Photochemically Driven Shape Changes of Crystalline Organic Nanorods

Rabih O. Al-Kaysi, Astrid M. Müller, and Christopher J. Bardeen*

Department of Chemistry, University of California, Riverside, California 92521

Received June 27, 2006; E-mail: christopher.bardeen@ucr.edu

A key goal of nanotechnology is the transformation of chemical energy into mechanical motion, for example, using photon energy to drive molecular displacements.^{1,2} Organic crystalline materials are of particular interest,³ and crystal-to-crystal photochemical transformations have been shown to be technologically useful.⁴ However, many chemical reactions that involve large-scale atomic motions, such as photodimerizations, do not lead to useful mechanical motion.^{5,6} This is because irradiating a molecular crystal induces a heterogeneous mixture of reacted and unreacted regions within the crystal.⁷ Reactant and product molecules migrate to their respective regions, and the resultant phase separation is often sufficiently violent to destroy the crystal. In this communication, we show that controlling the nanoscale morphology of organic molecular crystals can prevent the disintegration that usually accompanies photodimerization. Rods (200 nm diameter) composed of 9-*tert*-butylanthroate (9-TBAE) undergo a rapid [4 + 4] photodimerization⁸ that results in a 15% increase in rod length without the fragmentation. The uniform anisotropic expansion of these rods may hold promise for developing photoresponsive organic nanostructures.

The 9-TBAE was synthesized according to well-established literature procedures.⁹ The organic nanorods are obtained by solvent annealing in 200 nm Al₂O₃ templates,¹⁰ as recently described by Al-Kaysi et al.¹¹ The rods are deposited on a glass substrate and observed using fluorescence microscopy. Under 365 nm excitation, the nanorods emit a broad yellow–green emission, characteristic of anthracene excimer fluorescence. If the intensity is increased to 70 mW/cm², the rods undergo rapid bending and re-straightening over the course of a few seconds before they become stationary again. During this transformation, the 500 nm excimer emission is replaced by a new peak at 450 nm, characteristic of isolated 9-TBAE chromophores. Figure 1a shows fluorescence microscopy images of a bundle of rods before and after illumination. The rods have separated, and their length has increased by an average of 15%. This transformation can also be induced for rods still inside the Al₂O₃ membranes. Figure 1b,c shows that illumination causes the rods to expand out of the pores, disrupting the smooth surface layer and protruding up to 5 μm above the membrane surface. This photoinduced length change was observed for the 9-TBAE nanorods under a variety of preparation and isolation conditions. When random micron to millimeter size crystals of 9-TBAE were irradiated, they underwent the same color change but fragmented into smaller, irregularly shaped pieces instead of expanding uniformly.

The expansion of the rods along their long axis is accompanied by a contraction along their short axis. This contraction is too small to be observed in fluorescence microscopy images but can be measured using atomic force microscopy (AFM). Figure 2a,b shows the AFM image of a single rod fragment, isolated from an aqueous suspension after sonication and the addition of a surfactant (sodium dodecyl sulfate). After illumination, the length of the fragment increases by ~15%, consistent with the fluorescence images, but

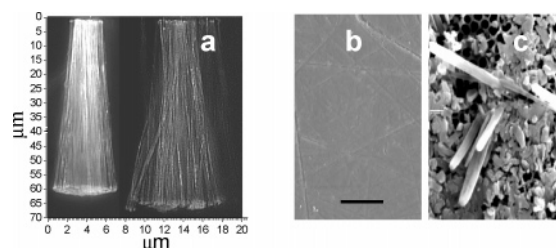


Figure 1. (a) Fluorescence image of a bundle of nanorods, before and after irradiation with 365 nm. The rods lengthen by an average of 15% as measured along a single rod. (b) SEM image of solvent-annealed 9-TBAE in the Al₂O₃ before illumination. (c) SEM image of the surface after illumination with 365 nm light. Scale bar is 600 nm.

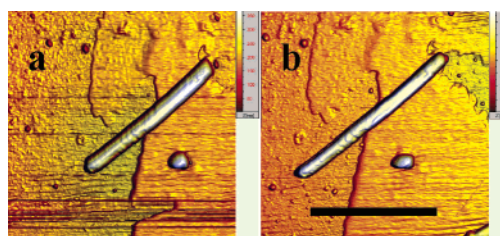


Figure 2. (a) AFM image of a single nanorod before illumination and (b) after illumination with 365 nm. Scale bar is 6 μm. Note that the diameter of the rod in the *xy* plane appears greater than 200 nm due to its convolution with the broad AFM tip.

the height of the SDS-coated rods decreases by 2–5%, depending on where along the rod the diameter is measured.

The anisotropic changes in rod shape suggest that the rods are composed of aligned molecules or are crystalline. To examine the molecular arrangement within the rods, we used transmission electron microscopy (TEM). TEM measurements on these materials are challenging since they decompose within a few seconds under electron beam exposure, but even with very short (2–4 s) exposure times, clear electron diffraction spots could be discerned in TEM images of isolated bundles. No diffraction rings, which would indicate a highly polycrystalline or amorphous material, were observed. Dark-field TEM on different regions of the same rod revealed single crystal domains of 0.5 μm or larger. Electron diffraction spots and crystalline domains were also observed for the rods after 365 nm irradiation, indicating that some degree of crystallinity is maintained after the photoreaction. The TEM measurements are consistent with our earlier results showing the solvent-annealed rods are composed of micron-scale single crystal domains.¹¹ These domains must be at least partially aligned to explain the anisotropic expansion we observe.

The above observations suggest that a crystal-to-crystal photodimerization plays a role in the observed shape changes. In order to gain insight into the molecular origin, we grew crystals of both the monomer and photodimer from solution and obtained their structures using X-ray diffraction. The partial crystal structure of monomeric 9-TBAE is shown in Figure 3a and is composed of a

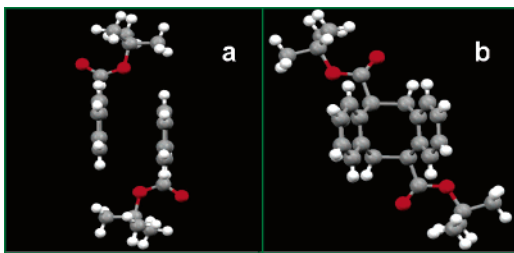


Figure 3. X-ray crystal structures of (a) monomer. The distance between the peripheral hydrogens of the *tert*-butyl group is 12.6 Å, and the shortest distance between the aromatic rings is 3.4 Å. (b) Dimer: Distance between the peripheral hydrogens of the *tert*-butyl groups is 14.2 Å, and the distance between the outer aromatic rings is 3.6 Å. The dimensions of the boxes in (a) and (b) are the same.

herringbone arrangement of dimers.¹² The face-to-face arrangement of the anthracene moieties, with the *tert*-butyl groups of neighboring anthracenes *trans* to each other, is known to facilitate efficient photodimerization.¹³ The photodimer could not be crystallized without inclusion of solvent molecules, but these fill the interstitial spaces and probably have little effect on the molecular packing. A more serious concern is whether the solvent-grown dimer crystals accurately reflect the structures generated by the solid-to-solid photodimerized nanorods. In general, solid-state photochemical reactions require significant reconstructive phase transitions.¹⁴ The powder X-ray diffraction patterns for the solution-grown crystals and the photodimerized nanorods show the same number and spacing of diffraction peaks, indicating that the solvent-grown crystal reflects the photogenerated dimer structure in the rods. The fact that the monomer and dimer crystals have different packing motifs indicates that the photodimerization drives a phase transition that alters the rod dimensions while preserving its morphology. Figure 3b shows that, although the cycloaddition has drawn the carbons on the central phenyl rings closer, the outer phenyl rings are actually spaced farther apart due to a ring puckering induced by loss of conjugation. Even more dramatic is the rotation of the *tert*-butyl groups from overlapping the neighboring anthracene ring to pointing in the opposite direction. The net effect is to increase the volume occupied per anthracene unit. X-ray diffraction determination of the crystal parameters confirms that the volume per anthracene moiety changes from 371 Å³ in the monomer crystal to 407 Å³ in the dimer crystal, an increase of 9.7%. Since the X-ray analysis was done on pure crystals, this volume change should provide an upper bound for what can be observed in the nanorods. The AFM measurements on individual rods yield a 15% increase in length accompanied by an average 3.5% decrease in radius, resulting in an overall volume increase of 7% for a single rod. This increase is slightly less than the 9.7% volume increase estimated from the crystal structures, probably because we do not photodimerize all of the monomers in a given rod. Evidence for incomplete conversion is provided by the blue monomer fluorescence, which originates from isolated, unreacted monomers trapped within the dimer crystal.¹⁵

Both the X-ray crystal structures and the AFM measurements are consistent with the photoinduced change in rod morphology being the result of a crystal-to-crystal photodimerization. It is an open question as to why that this photochemical transformation does not lead to fragmentation in the rods as it does in the unshaped crystals. Photochemical reactions in organic crystals are known to

generate large strain energies.^{16,17} Since the crystal layers at the surface can relax more easily, the high surface-to-volume ratio of the rods leads to a mechanism for strain relief that is absent in larger crystals. This mechanism has been inferred from the epitaxial growth of inorganic crystal layers¹⁸ but not in organic materials to our knowledge.

In earlier work on spiroopyran single crystals,¹⁹ it was determined that 600 layers were required to undergo photoisomerization to produce a reversible crystal expansion of 1 monolayer. Thus the photoinduced change in the crystal dimensions was 0.16%, almost 2 orders of magnitude smaller than that in the 9-TBAE rods. We have made preliminary attempts to examine the reversibility by using short wavelength UV light in an attempt to photodissociate the dimers. Irradiating the dimerized nanorods with 254 nm light caused a slight ~3% decrease in length, but even after extended illumination (>1 h), the rods did not shrink back to their original dimensions, and the yellow excimer fluorescence did not reappear. Additional work is needed to determine the degree of reversibility.

We have shown how crystalline organic nanorods can undergo large length changes upon photodimerization. While this photochemistry typically leads to the fragmentation of 9-TBAE crystals, the nanorods retain their shape and integrity. The ability of the rods to survive the crystal-to-crystal transition is likely due to their nanoscale dimensions, which maximize the surface-to-volume ratio and provide a way to relieve the crystal strain induced by the photoreaction. This phenomenon may provide a general way to harness the power of organic solid-state photochemistry to do work on the nanometer scale.

Acknowledgment. This work was supported by the NSF, Grant CHE-0517095, and the Central Facility for Advanced Microscopy and Microanalysis (CFAMM) at UCR.

Supporting Information Available: Synthesis of 9-TBAE and the photodimer, with the crystallographic information, CIF files, AFM, SEM, and TEM experimental conditions are available. This material is available free of charge via the Internet at <http://pubs.acs.org>.

References

- Balzani, V.; Clemente-Leon, M.; Credi, A.; Ferrer, B.; Venturi, M.; Flood, A. H.; Stoddart, J. F. *Proc. Natl. Acad. Sci. U.S.A.* **2006**, *103*, 1178–1183.
- Feringa, B. L.; van Delden, R. A. v.; Koumura, N.; Geertsema, E. M. *Chem. Rev.* **2000**, *100*, 1789–1816.
- Khuong, T.-A. V.; Nunez, J. E.; Godinez, C. E.; Garcia-Garibay, M. A. *Acc. Chem. Res.* **2006**, *39*, 413–422.
- Papaefstathiou, G. S.; Zhong, Z.; Geng, L.; MacGillivray, L. R. *J. Am. Chem. Soc.* **2004**, *126*, 9158–9159.
- Enkelmann, V. *Mol. Cryst. Liq. Cryst.* **1998**, *313*, 15–23.
- Kaupp, G. *Angew. Chem., Int. Ed.* **1992**, *31*, 595–598.
- Turowska-Tyrk, I. *J. Phys. Org. Chem.* **2004**, *17*, 837–847.
- Shon, R. S.-L.; Cowan, D. O.; Schmiegel, W. W. *J. Phys. Chem.* **1975**, *79*, 2087–2092.
- Parish, R. C.; Stock, L. M. *Tetrahedron Lett.* **1964**, 1285–1288.
- Martin, C. R. *Science* **1994**, *266*, 1961–1966.
- Al-Kaysi, R. O.; Bardeen, C. J. *Chem. Commun.* **2006**, 1224–1226.
- Sweeting, L. M.; Rheingold, A. L.; Gingerich, J. M.; Rutter, A. W.; Spence, R. A.; Cox, C. D.; Kim, T. J. *Chem. Mater.* **1997**, *9*, 1103–1115.
- Cohen, M. D. *Angew. Chem., Int. Ed.* **1975**, *14*, 386–393.
- Keating, A. E.; Garcia-Garibay, M. A., Eds. *Photochemical Solid-to-Solid Reactions*, 1 ed.; Dekker: New York, 1998; Vol. 2, pp 195–248.
- MacFarlane, R. M.; Philpott, M. R. *Chem. Phys. Lett.* **1976**, *41*, 33–36.
- McBride, J. M.; Segmuller, B. E.; Hollingsworth, M. D.; Mills, D. E.; Weber, B. A. *Science* **1986**, *234*, 830–835.
- Peachey, N. M.; Eckhardt, C. J. *J. Phys. Chem.* **1993**, *97*, 10849–10856.
- Snyder, C. W.; Orr, B. G.; Kessler, D.; Sander, L. M. *Phys. Rev. Lett.* **1991**, *66*, 3032–3035.
- Irie, M.; Kobatake, S.; Horichi, M. *Science* **2001**, *291*, 1769–1772.

JA064535P